Available online at www.sciencedirect.com
ScienceDirect
Journal of Magnetic Resonance 182 (2006) 200–207
JMR Journal of Magnetic Resonance
www.elsevier.com/locate/jmr

Using metamaterial yokes in NMR measurements

Mathieu Allard *, R. Mark Henkelman

Mouse Imaging Centre, Hospital for Sick Children, Toronto, Ont., Canada M5G 1X8

Received 18 April 2006; revised 22 June 2006
Available online 21 July 2006

Abstract

Swiss rolls are one instance of metamaterials, and can be described as an effective medium with a complex, anisotropic magnetic permeability. It has been shown that bundles of Swiss rolls can guide the magnetic flux in magnetic resonance measurements and increase the coupling between the nuclear spins and the receiver coil. Here, we investigate, with a numerical model, whether Swiss rolls can boost the detected signal in a NMR experiment, where the rolls could provide a low-reluctance return path for the magnetic flux when shaped in a yoke encircling the sample. The system consisting of the nuclear spin, the rolls and the receiver coil is analyzed with the method of finite differences in time domain (FDTD). The results show that small gains in the received signal are possible, but only if the losses (resistive and dielectric) in the rolls are reduced by over one order of magnitude from their present value in state-of-the-art materials. This situation arises because of the energy dissipation in the rolls and the mode splitting caused by the coupling between the rolls and the resonant coil.

Keywords: Metamaterials; NMR spectroscopy; Negative refraction; Swiss rolls

1. Introduction

A metamaterial is an array of small elements that interact with electromagnetic fields. Since the characteristic dimensions of the elements are smaller than the wavelength by at least an order of magnitude, a metamaterial can be approximately described as an effective medium. One point of interest in metamaterials is that strong magnetic properties can be engineered at gigahertz frequencies, where strong magnetic phenomena are rare in classical materials [1]. The possibility of having a negative index of refraction, when both the effective permittivity and permeability are negative, has attracted considerable attention [2,3]. This has been proposed as a basis for a perfect lens. Smith et al. [4] and Ramakrishna [5] provide comprehensive and recent reviews of the field.

In the context of magnetic resonance, it has been demonstrated that metamaterials, specifically the so-called "Swiss rolls," can guide high-frequency magnetic flux. These structures, first proposed by Pendry [1] and later manufactured by Wiltshire et al. [6], are made by rolling sheets of conductor and insulator around a mandrel. It was shown that bundles of Swiss rolls can carry the magnetic flux from its source to a distant receiver coil. This has potential to help with imaging [7]. It should be noted that, in the context of magnetic resonance, imaging is accomplished by spatial encoding and metamaterials do not play the role of a lens. Instead, they manipulate the magnetic flux produced by the magnetic dipoles (spins) to facilitate detection. Accordingly, the magnetic resonance applications proposed to date rely exclusively on the effective permeability of metamaterials, with the permittivity playing only a marginal role.

In order for metamaterials to guide and concentrate the magnetic flux generated by a dipole, they should in fact have an effective permeability as high as possible. The real part of the highest permeability reported so far is 17 [7]. One way to exploit this would be to provide for the flux a low-reluctance return path that intercepts a receiver coil: this would boost the power of the detected signal [8,9]. Since magnetic resonance imaging and spectroscopy are

* Corresponding author. Fax: +1 416 813 2208.
E-mail address: mallard@sickkids.ca (M. Allard).

1090-7807/$ - see front matter © 2006 Elsevier Inc. All rights reserved.
doi:10.1016/j.jmr.2006.06.029

generally limited by the signal-to-noise ratio, any improvement in signal is desirable. Fig. 1 illustrates the concept. Here, the metamaterial would perform a role analogous to that of ferromagnetic cores in transformers, which increase the coupling between the primary and the secondary windings. Whereas ferromagnetic materials cannot be used in a MR setting since they interact strongly with the static B_0 field, non-ferromagnetic metamaterials can safely be used because their DC permeability is essentially unity. Drawing from the basic design of transformers, a simple method of using metamaterials is to position a yoke around the sample to be analyzed. If the resonance frequency of metamaterials is chosen to be slightly above the Larmor frequency, the permeability (its real part) would be larger than one and some of the magnetic flux could be diverted from its original path to run along the length of the yoke and around the receiver coil.

Despite the initial interest in using metamaterials in MR experiments, there has not yet been a clear analysis or a demonstration of the gains that they could provide. In this article, we investigate, through *ab initio* numerical simulations, how metamaterials consisting of Swiss rolls interact with the magnetic field generated by a spin and by receiver coils. The electromagnetic calculations deal with spatially averaged fields but, instead of considering the metamaterial as an effective magnetic medium, they directly compute, along with the time varying fields, the charge and currents sustained by the rolls. The goal here is to provide a reliable estimate of the gain that can be achieved for rolls with a given quality factor, and to determine what are the relevant geometric factors influencing that gain.

Section 2 presents in detail the numerical model used in the simulations. Section 3 presents the results obtained with the model and Section 4 discusses the prospects of how useful metamaterials could be in this particular application and the requirements that it puts on the Swiss rolls fabrication.

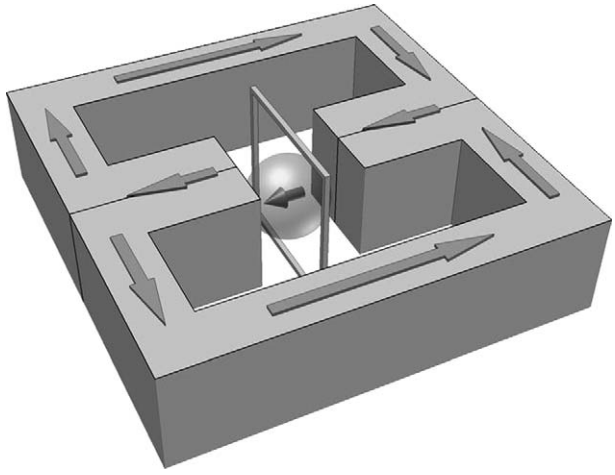

Fig. 1. Metamaterial yoke guiding the magnetic flux around a receiver coil. The sample, shown as a sphere, is placed in a gap in the center of the yoke, and is surrounded by a receiver coil shaped as a square loop. The arrows show the magnetic flux.

2. Model

2.1. Structure and electromagnetic behavior of swiss rolls

A Swiss roll is made of a thin conducting foil and an insulating sheet rolled on a mandrel of radius r (see Fig. 2). The conducting foil can support a current in the roll cross-section; this current is expressed per unit length of roll, and is denoted j_s. Such a current generates a longitudinal magnetic field inside the roll; thus, the roll has an inductance L_s, inversely proportional to the its length. When a current circulates around the roll, a charge q_s accumulates on the first and last turns of conducting foil: the roll also has a capacitance per unit length C_s. Therefore, the roll is in effect a resonant RLC circuit which can be described by its resonant frequency ω_0 and quality factor Q. The resistance is a combination of a series resistance due to the finite conductance of the foil and a parallel resistance due to the finite resistance of the dielectric. Without loss of generality, we assume that all losses come from the parallel resistance R_p. The properties of the rolls are then:

$$L_s = \mu_0 \pi r^2 (N-1)^2, \tag{1}$$

$$C_s = \frac{\epsilon_0 \epsilon_r 2\pi r}{d(N-1)}, \tag{2}$$

$$R_p = \frac{d(N-1)}{2\pi r} \rho_{diel}, \tag{3}$$

$$\omega_0 = \frac{1}{\sqrt{L_s C_s}} = \sqrt{\frac{d c_0^2}{2\pi^2 r^3 (N-1)\epsilon_r}}, \tag{4}$$

$$Q = \frac{\omega_0}{\Delta\omega} = \frac{R_p}{\omega_0 L_s} = \frac{\rho_{diel}}{\eta_0} \sqrt{\frac{d\epsilon_r}{2\pi r^3 (N-1)}}, \tag{5}$$

where d is the thickness of the insulating sheet, N is the number of turns in the roll, r is the radius of the mandrel, ρ_{diel} is the resistivity of the dielectric, c_0 is the speed of light and η_0 is the impedance of vacuum. Eq. (1) is strictly true only for an isolated long roll, as coupling to other nearby

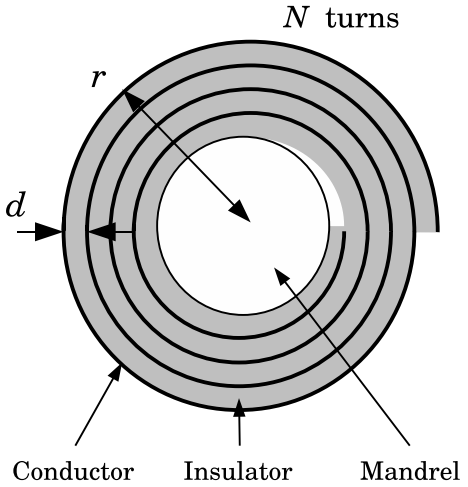

Fig. 2. Cross-section of a Swiss roll.

rolls (as when a roll is part of a bundle) can change the inductance [10]. The approximation is still good, however, for long and narrow bundles and for the yokes discussed here.

As shown by Pendry [1], Swiss rolls become effectively "magnetized" under the influence of an external magnetic field at a frequency close to ω_0. A bundle of Swiss rolls can therefore be described as an effective medium with a frequency-dependent, anisotropic permeability. At resonance ($\omega = \omega_0$), the longitudinal component of the permeability can be shown to be $\mu_{\text{eff}} = 1 + jFQ$ (F is the volume fraction occupied by the rolls); the real part of the permeability reaches a maximum, just below resonance, of $1 + FQ/2$. In our *ab initio* model, however, we maintain the charge and current description of the rolls rather than using the effective medium description.

As with any conductor, external electric fields will interact with the Swiss rolls by causing charges to appear on their outer surfaces. No electric field can exist inside any roll, since the conducting foil will shield any external field. A bundle of non-contacting rolls, however, will become electrically polarized when subjected to a transverse electric field. This effect is not resonant and is not accompanied by any significant loss. It can therefore be accounted by assigning a real, larger-than-one effective permittivity for the bundle.

2.2. Governing equations of the model

Here, we present the algebraic and differential equations governing the electric and magnetic fields, as well as the current and charge supported by the Swiss rolls. Once all these quantities are discretized in space and in time, a set of numerical time-update equations is obtained, with which the temporal evolution of all physical quantities can be computed explicitly.

The equivalent electrical circuit of a Swiss roll is shown in Fig. 3. From now on, we assume that the Swiss roll lies along the x axis. In this parallel RLC circuit, the electromotive force is equal to the voltage across the foils:

$$\frac{L_s}{N-1}\frac{\partial H_x^{\text{in}}}{\partial t} + \frac{q_s}{C_s} = 0, \tag{6}$$

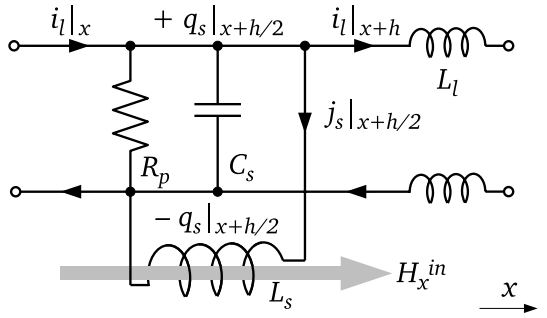

Fig. 3. Electrical circuit describing a unit length of Swiss roll.

where H_x^{in} is the field component inside and along the axis of the roll. Swiss rolls can also support opposing longitudinal currents, i_l, on the innermost and outermost turns of the foil; in that, they act as a transmission line, governed by the following equations:

$$\frac{\partial q_s}{\partial t} - j_s - \frac{\partial i_l}{\partial x} = 0, \tag{7}$$

$$\frac{1}{C_s}\frac{\partial q_s}{\partial x} + L_l\frac{\partial i_l}{\partial t} = 0. \tag{8}$$

The longitudinal inductance per unit length, L_l, is that of a coaxial cable:

$$L_l = \frac{\mu_0}{2\pi}\ln\left(\frac{r + d(N-1)}{r}\right) \approx \frac{\mu_0(N-1)d}{2\pi r}. \tag{9}$$

The approximation applies as a long as $d(N-1) \ll r$.

Since we want to include the electric and magnetic fields outside of the Swiss rolls in the model, we must add Maxwell's equations to the list of governing equations. The Swiss rolls do not support any unpaired charge, therefore there is no need to include Maxwell's divergence equations in the model. The curl equations are here expressed in integral form:

$$\oint \vec{H}\cdot\vec{dl} = \int \epsilon\frac{\partial \vec{E}}{\partial t}\cdot\vec{ds} + \vec{i}\cdot\hat{s}, \tag{10}$$

$$\oint \vec{E}\cdot\vec{dl} = -\int \mu\frac{\partial \vec{H}}{\partial t}\cdot\vec{ds}. \tag{11}$$

Here, $\vec{dl}$ denotes a length element along a closed path and $\vec{ds}$ a surface element on the surface delimited by the closed path. In the above equations, μ is the microscopic, not the effective, permeability, and is therefore identically equal to μ_0. $\vec{i}$ is a directed current, and may include the current supported by the Swiss rolls, depending on the path over which the integral is evaluated. The permittivity, ϵ, will take an effective value in the Swiss roll bundle, and be set to ϵ_0 elsewhere.

2.3. FDTD model

We use the well established method of *finite differences in time domain* (FDTD) to solve the governing equations [11,12]. In FDTD, the electric and magnetic fields are discretized in space, on two interpenetrating simple cubic lattices, as shown in Fig. 4, and in time, on alternating time steps. The integrals in Eqs. (10) and (11) are evaluated on a square loop, and are approximated by finite differences. For example, Eq. (11), when evaluated on a square oriented along $\hat{z}$ and centered at a point (x,y,z,t), becomes

$$\begin{aligned}&\frac{1}{h_x}[E_y(x+h/2,y,z,t) - E_y(x-h/2,y,z,t)]\\ &\quad - \frac{1}{h_y}[E_x(x,y+h/2,z,t) - E_x(x,y-h/2,z,t)]\\ &= \frac{\mu_0}{\delta t}[H_z(x,y,z,t+\delta t/2) - H_z(x,y,z,t-\delta t/2)],\end{aligned} \tag{12}$$

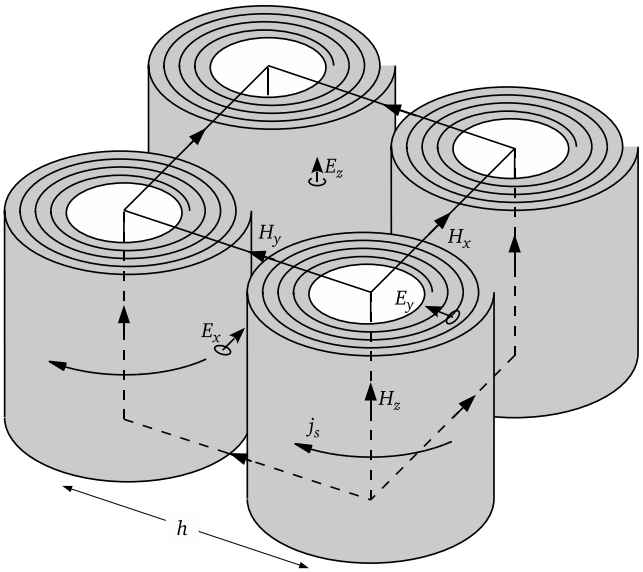

Fig. 4. Position of the FDTD grid and the field components with respect to the Swiss rolls.

where h_x h_y are the lattice constants and δt is the time step. To avoid unwieldy equations in the rest of this section, we introduce the finite-difference operators Δ_x, Δ_y, Δ_z and Δ_t, and rewrite the previous equation as

$$\frac{\Delta_x[E_y]}{h_x} - \frac{\Delta_y[E_x]}{h_y} = \frac{\mu_0 \Delta_t[H_z]}{\delta t}. \tag{13}$$

Six such equations can be derived, one for each of the six field components.

We assume that the Swiss rolls are microscopic elements, that is, we average the fields over the transverse size of the rolls. Therefore, we set the FDTD lattice constant to be exactly equal to the spacing between the rolls. Positioning the lattice as shown in Fig. 4 ensures that the closed-path over which the integral of Eq. (11) is evaluated does not cross the wall of a roll, a good thing because the electric field inside the rolls must be zero.

The magnetic fields inside and outside a roll are related by

$$H_x^{\text{in}} - H_x^{\text{out}} = (N-1) j_s. \tag{14}$$

When laying out the finite-difference equations for the components E_y and E_z, we must add terms accounting for the currents flowing in the two rolls intercepted by the integral surface. This is easily done by storing in memory the value of $H_x^{\text{out}} = H_x^{\text{in}} - (N-1) j_s$ rather than H_x^{in}: then, the current terms disappear from Eq. (10).

The only finite-difference equation that is modified from its original FDTD form is the one for H_x. The surface integral (right-hand side of Eq. (11)) must take into account the difference in magnetic field inside and outside of the roll:

$$\begin{aligned} \mu_0 \frac{\partial}{\partial t} \int H_x \mathrm{d}s &\approx \frac{\mu_0}{\delta t} \Delta_t \left[F H_x^{\text{in}} + (1-F) H_x^{\text{out}} \right] \\ &= \frac{\mu_0}{\delta t} \Delta_t \left[H_x^{\text{out}} + F(N-1) j_s \right], \end{aligned} \tag{15}$$

where $F = \pi r^2 / h^2$.

We now have all the equations governing the temporal evolution of the fields, currents and charges. By defining $\vec{H}$, j_s and i_l at integer time steps and $\vec{E}$ and q_s at half time steps, we can derive a set of explicit time-update equations for all nine scalar quantities in each FDTD cell. The equations are given in Appendix A.

2.4. General setup of simulations

The general setup of the simulation is a 3D orthogonal grid in which a magnetic dipole is placed at the center and is surrounded by Swiss rolls arranged as a yoke, and by a receiver coil shaped as a square loop (see Fig. 5).

Because of the symmetry of the setup along all three axes, the simulation domain is restricted to only one octant. The grid spacing, h, is taken to be unity everywhere except close to the outer boundaries, where it follows a geometric progression (with a ratio of 1.125). For all simulations presented in this article (except where otherwise stated), the grid comprises $60 \times 60 \times 60$ elements, with the inside $40 \times 40 \times 40$ elements having unity dimensions. The time step is taken to be $0.5h/c_0$ to satisfy the Courant's stability condition [11,12], and the total simulation time is taken to be long enough to allow the energy to fully decay in the rolls and in the receiver coil. In all simulations presented here, the resonance frequency of the rolls and of the receiver coil is chosen to be $0.002c_0/h$, for a wavelength of $500h$.

It must be noted that the time step here is not limited by the required temporal resolution, since the period of the dipole oscillation is 1000 times larger than the time step. Implicit techniques, which are not restricted by Courant's

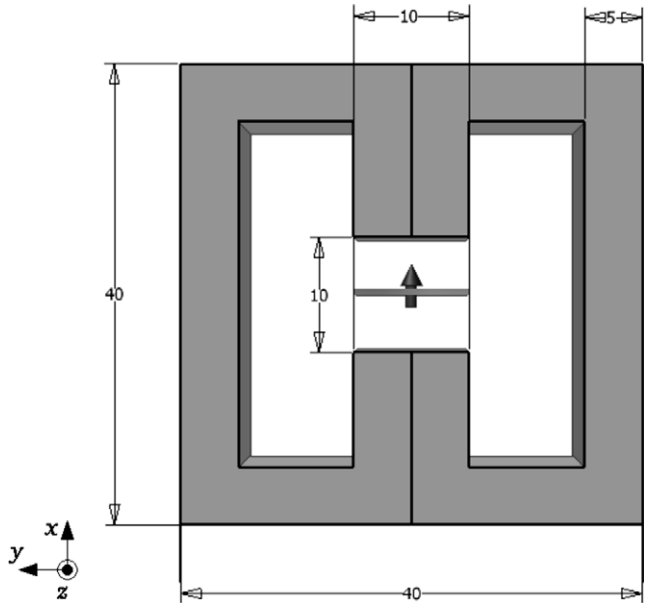

Fig. 5. General setup of the simulation. The dipole (arrow) and the coil can be seen at the center. The thickness of the yoke is 10. All dimensions are expressed in units of the FDTD grid (h).

stability criterion, could therefore offer great savings in computation time. The alternating direction implicit FDTD algorithm (ADI-FDTD) [12,13], however, was found to be inapplicable to this problem because the large spatial derivatives of the fields in the vicinity of the dipole lead to large numerical errors. This was discussed by Garcia et al. [14].

The magnetic dipole is implemented by adding a term to the H_x field component at the origin O at every time step:

$$H_x|_O^{n+1} = H_x|_O^n + [E_y \quad \text{and} \quad E_z \quad \text{terms}] - (M^{n+1} - M^n), \tag{16}$$

$$\begin{aligned} M^n &= \exp\left[-\left(\frac{n\delta t - t_{\text{offset}}}{T_{\text{duration}}}\right)^2\right] \sin(\omega_0 n\delta t) \\ &= \exp\left[-\left(\frac{0.5n - 900}{150}\right)^2\right] \sin\left(\frac{\pi n}{500}\right) \end{aligned} \tag{17}$$

The receiver coil (designated as Rx in the equations to follow) is described by its geometry, its resonance frequency ω_0, and its quality factor Q_{Rx}. It is implemented as a square loop of perfectly conducting wire (along which the electric field is always set to zero) in which is placed a leaky capacitor. The FDTD equations that govern the current and the charge in the coil are similar to those that apply to the rolls, and need not be repeated here.

The Swiss rolls are laid out around the central dipole. At 90° corners in the rolls, the inner and outer foils of the X-oriented section are assumed to be in electrical contact with those of the Y-oriented section. Thus, the longitudinal current i_l can flow freely along the entire length of the yoke. Otherwise, the X- and Y-oriented sections are considered to be independent rolls. We found this purely electric coupling between sections to be sufficient to prevent any leakage of the flux at the junctions (see Section 4).

First-order Mur's absorbing boundary conditions [12,15] are used at the outer boundaries of the simulation domain to limit reflections. Since only the near, evanescent field plays any significant role, the choice of boundary conditions is largely irrelevant, and there is no advantage to using Bérenger's perfectly matched absorbing layers [16,17], which ordinarily offer superior performance but with a large penalty in computation time.

3. Results

Several series of simulations were carried out to study separately how each of the parameters describing the metamaterial yoke and receiver coil affected the power of the received signal. All these simulations were carried out in relation to a standard case where the quality factor of both the Swiss rolls and the receiver coil was the same; we chose $Q = 100$, which is typical for MR probes and slightly better than the best reported value for Swiss rolls ($Q = 60$). The full outer dimensions of the yoke were $40 \times 40 \times 10$ unit cells, and the cross-section of the middle section of the yoke was 10×10. Note that these dimensions were smaller than the wavelength by a factor of more than 10, ensuring that the near-field case was maintained. To maximize the received signal, the gap width and the lateral size of the receiver coil should be as small as possible; both were taken to be 10 unit cells, a fair case if we assume that the sample dimensions are the same in all directions. All size and frequency units are consistent; the physical dimensions are uniquely determined by the choice of the Larmor frequency, itself determined by the strength of the static magnetic field.

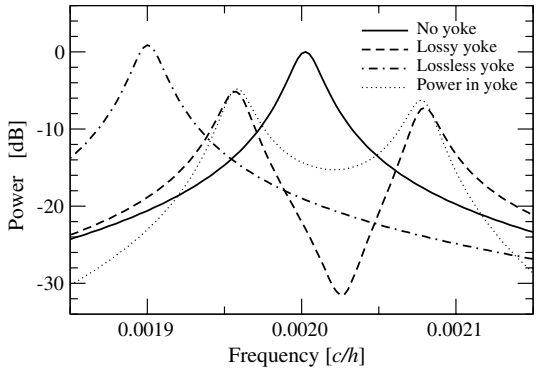

Fig. 6. Spectra of the power in the receiver coil, for the cases where the yoke is present, absent, or replaced with a lossless magnetic yoke (as described in text). The reference level (0 dB) is taken to be the peak power for the case without the yoke present. The spectrum of the total power dissipated in the rolls is also shown.

The useful output of the FDTD simulation is the spectrum of the power detected in the receiver coil: it is shown in Fig. 6 along with the power spectrum in the case where the yoke was absent. Also shown is the spectrum of the power dissipated in the rolls. Whereas the spectrum where only the coil is present exhibits a single peak at a frequency of $0.002c_0/h$, the peak is split in two when both the coil and the yoke are present. This confirms that the two elements are inductively coupled. It is obvious from Fig. 6 that, with the parameters chosen here, there is a net loss of -5.1 dB in the received signal when the yoke is present.

To investigate the cause of this loss, we ran another simulation where the Swiss rolls were replaced by a lossless non-resonant magnetic material, which had a real, frequency-independent anisotropic permeability with components $\mu_\perp = 1$ and $\mu_\parallel = 50$, the latter being approximately equal to the peak value for Swiss rolls with $Q = 100$. The resulting power spectrum in the coil is also plotted in Fig. 6. It features a small but positive gain of $+1.0$ dB. The large shift in resonant frequency is caused by a change in the receiver coil inductance due to the proximity of the magnetic yoke. All this points to losses in the Swiss rolls as the culprit for the loss in signal. More will be said about the impact of the losses in Section 4.

3.1. Effect of quality factor

We investigated the effect of the quality factor of the Swiss rolls, Q_{roll}, on the received signal. Fig. 7 shows the

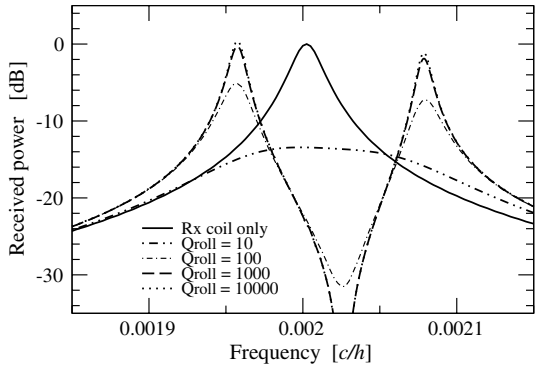

Fig. 7. Received power spectra for different values of Q_{roll}. In all cases, $Q_{Rx} = 100$.

spectra of the received signal for $Q_{roll} = 10$, 100, 1000 and 10,000. The peak power of the received signal increases with Q_{roll}; we found that, when $Q_{roll} \approx 1500$, it reaches about the same value as in the case where the rolls are absent. When $Q_{roll} = 10{,}000$, the received signal gains +0.4 dB over the coil-only case; increasing Q_{roll} further yields no significant additional gain.

Another series of simulation was carried out with equal values of Q_{roll} and Q_{Rx} ranging from 10 to 1000, to see how the penalty in the received signal changed with the quality factor. Finally, simulations with lossless yokes with a permeability ranging from 5 to 500 were also carried out. All results are summarized in Fig. 8, where only the peak power is plotted against Q.

From these results, it is clear that, whereas the (hypothetical) lossless magnetic yokes always lead to a modest gain (up to +1.3 dB at $\mu = 250$), yokes made of Swiss rolls will only bring a gain when their quality factor is at least fifteen times as high as the quality factor of the receiver coil. It also appears that the penalty incurred by using a yoke with the same Q as the receiver coil is about 5 dB and is independent of that Q.

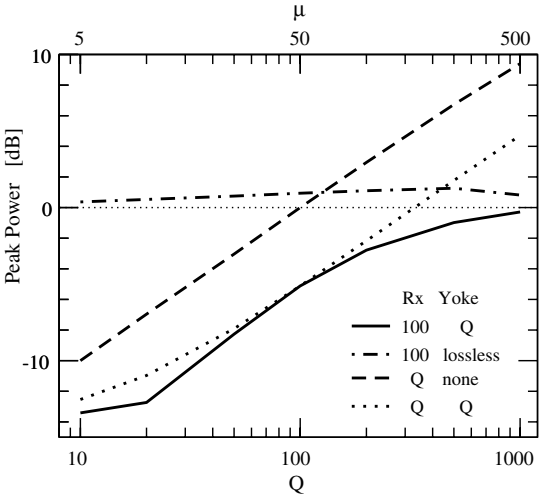

Fig. 8. Peak power as a function of the quality factor. Four cases are presented: (i) fixed Q_{Rx}, variable Q_{roll}; (ii) fixed Q_{Rx}, lossless yoke with variable permeability μ; (iii) variable Q_{Rx}, no yoke present; (iv) variable but equal Q_{Rx} and Q_{roll}. The thin dotted line marks the 0 dB reference case, corresponding to the peak power received with a coil alone with $Q_{Rx} = 100$.

3.2. Effect of yoke geometry

Although the quality factors of the yoke and receiver coils have the strongest influence on the received power, the geometries of the yoke and the coil also affect it. We carried out a series of simulations where we varied the overall length of the yoke, the width of the gap in which the sample is placed, the cross-section of the yoke, and the size of the receiver coil. In all cases, the quality factors are $Q_{roll} = 10{,}000$ and $Q_{Rx} = 100$, which ensures that there is a small positive gain. Since the spectra of the received signal are all similar to the one shown in Fig. 6, we list in Table 1 only the peak powers.

The main effect of changing the geometry of the yoke is to change the strength of the coupling between the rolls and the receiver coil. As the coupling becomes stronger, the frequency splitting between the two modes increases. The gain also increases with the coupling strength but the changes are small. The quality factor is thus by far the most important parameter affecting the received signal.

A greater overall length of the rolls in the yoke is seen to decrease the coupling strength because the total reluctance of the yoke increases with its length. Increasing the width of the gap in the yoke also rapidly decreases coupling. Finally, increasing the gap cross-section increases coupling marginally. These findings are all consistent with the concept of the Swiss rolls being conduits for the magnetic flux.

The size of the receiver coil also strongly affects the signal, as a smaller coil will couple more strongly with the

Table 1
Peak received power for several yoke and coil geometries

Description	$X = Y$	G	$W = Z$	W_{Rx}	P_{max} [dB]	Δf_{mode} [$\times 10^{-6} c_0/h$]
Reference cases	—	—	—	10	0.0	—
(coil alone)	—	—	—	20	−10.3	—
	—	—	—	28	−15.5	—
Outer dimensions	40	10	10	10	0.4	123
	60[a]	10	10	10	0.3	94
	80[a]	10	10	10	0.2	80
Gap in yoke	40	10	10	10	0.4	123
	40	20	10	10	0.2	59
	40	28	10	10	0.1	46
Cross-section	40	10	6	10	0.3	80
	40	10	10	10	0.4	123
	40	10	18	10	0.3	154
Coil size	40	10	10	10	0.4	123
	40	10	10	20	−8.4	156
	40	10	10	28	−12.3	151

X, Y, full outer dimensions of yoke; G, width of the central gap in the yoke; W, width of the center bar of yoke; Z, full thickness of yoke; W_{Rx}, width and height of receiver coil; P_{max}, peak power; Δf_{mode}, mode splitting.

[a] The FDTD grid was extended to $80 \times 80 \times 80$ cells in these simulations.

spin. As the size of the coil increases, the advantage in using Swiss rolls becomes greater.

4. Discussion

As shown in the previous section, the only way to incur a gain by using a metamaterial yoke is to increase its quality factor to at least 15 times the quality factor of the receiver coil. In other words, the resistive and dielectric losses in the Swiss rolls must be reduced. Modifying the geometry of the yoke, although it affects the coupling strength, does not change this situation. In this section, we discuss further the implications of the losses in the rolls.

It is important to note that there is almost no leakage of magnetic flux from the rolls. This can seen in Fig. 9, which shows the variation of the internal magnetic field along the full length of a roll. In the low-frequency mode, the field varies by only 5% along the length of the roll, as the small losses let some of the flux out. The longitudinal field is also remarkably continuous across the 90° bends. In the high-frequency mode, the field is actually greater away from the roll extremities. This is due to the field generated by the coil, which is out of phase (in this mode) with the field generated by the transverse current in the roll and interferes destructively with it. These findings confirm that the rolls do effectively guide the magnetic flux.

There are two reasons why the detected signal power is reduced when the metamaterial yoke is introduced in the system. First, the resonance mode is split in two, and, in a true MR experiment, the narrow-band dipole can couple to only one of the modes. There is therefore a net reduction of signal when the rolls are present, by a factor of close to 0.5 (−3 dB). Second, when the quality factors are equal, half the energy is dissipated in the rolls where it does not contribute to the detection. This causes a further loss, also of about −3 dB, in each of the two modes. If there was no direct coupling between the magnetic dipole and the yoke, the loss in each mode would have been about −6 dB; the fact that the loss in the symmetric (lower-frequency) mode is only −5.1 dB proves that this coupling exists.

To provide a gain in received signal, the losses in the rolls must be reduced, and the coupling between the metamaterial yoke and the receiver coil must be raised as high as possible so that the dipole couples only to the symmetric mode. To find how much gain can ultimately be achieved, we can look at the case of a lossless and non-resonant yoke, for which no loss and no mode splitting exist, and increase its permeability to infinity. This calculation cannot be easily done with FDTD, due to magnetic resonances inherent to the yoke. Instead, we previously carried out a similar quasi-static calculation [9] and found that, with essentially the same geometry, the gain increases with the permeability and reaches a limit value of 2.2 dB for $\mu_{\text{eff}} \gtrsim 1000$. With this in mind, we find that there should not be a fundamental reason to preclude net gains by using metamaterials yokes, but the requirements put on the manufacturing of the Swiss rolls are rather high and significantly above what has been achieved to date.

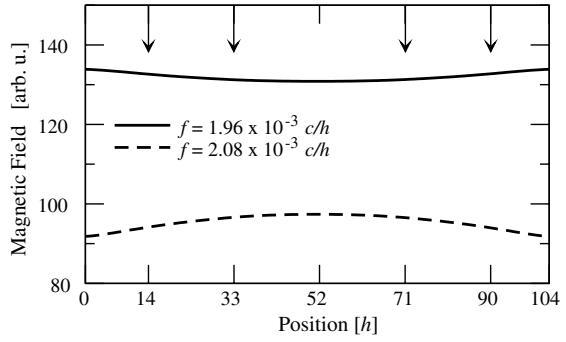

Fig. 9. Longitudinal magnetic field inside a roll along its length. The arrows denote the position of the 90° bends in the roll.

Reducing the losses in the rolls would increase the signal in two ways. First, most of the energy would then be dissipated in the coil where it can be detected. This would eliminate up to 3 dB of losses. Second, a higher quality factor implies a higher effective permeability and a stronger coupling to the dipole which would offset the loss caused by the mode splitting.

The coupling between the metamaterial yoke and the receiver coil (as well as between the yoke and the dipole) can be increased also by changing the geometry of the system. One way would be to wrap the coil around the yoke itself instead of around the sample. Moving the coil is not desirable, however, because the direct coupling to the dipole and therefore the received signal would be reduced considerably. The coil must remain as close to the sample as possible, thus the mode splitting is unavoidable. Instead, we must focus on optimizing the geometry of the yoke alone. A marginal gain increase could be possible by wrapping the yoke more tightly around the sample, but we expect the geometry described here to be close to the best case possible, as long as we keep the fair hypothesis that the sample is spherical and that the coil diameter and the gap width in the yoke must be equal.

One interesting possibility to reduce resistive losses is to use a superconducting foil in the Swiss rolls [18]. Since most MR imagers and spectrometers already use superconductors immersed in liquid helium to produce the magnetic fields, it should be possible to place a metamaterial in the cryostat that is already present.

Even if the present level of losses in Swiss rolls preclude the application anticipated in this article, other interesting uses may still be found for them in magnetic resonance experiments. Because Swiss rolls do not leak magnetic flux, they can be made to be completely uncoupled from each other even when in a bundle. This has some potential in spatial encoding with multiple rolls.

5. Conclusion

Here, we have reported *ab initio* simulations of how bundles of Swiss rolls interact with the fields generated

by a magnetic dipole and a receiver coil, and considered whether they could improve the detection efficiency in a magnetic resonance measurement. We found that gains are possible only if losses are substantially reduced, by more than one order of magnitude, from where they stand at the moment. Further optimization of the geometry of how the roll and the receiver coils are laid out is not expected to impact this situation significantly.

Other applications may exist where the present-day losses in Swiss rolls are acceptable. But in any case, it is important to remember that these materials are not simply conduits for the magnetic flux: they also absorb and dissipate energy and actively couple to other resonating elements. This must be taken into account when designing applications of metamaterials in magnetic resonance.

Acknowledgments

We thank M.C.K. Wiltshire, J.V. Hajnal and I.R. Young for stimulating discussions. M. Allard acknowledges the financial support of the Natural Science and Engineering Research Council of Canada. R.M. Henkelman holds a Canada Research Chair in Imaging.

Appendix A. Time-update equations

Here, we assume, as before, that we are in a region of space occupied by a Swiss roll oriented along $\hat{x}$. The update equations, obtained by expanding the differential equations into finite differences in time and in space, are as follows. Keeping the finite-difference operators (Eq. (13)),

$$E_x^{n+\frac{1}{2}} = E_x^{n-\frac{1}{2}} + \frac{\delta t}{\epsilon_{xx}}\left(\frac{\Delta_y[H_z^n]}{h_y} - \frac{\Delta_z[H_y^n]}{h_z}\right) \tag{18}$$

$$E_y^{n+\frac{1}{2}} = E_y^{n-\frac{1}{2}} + \frac{\delta t}{\epsilon_{yy}}\left(\frac{\Delta_z[H_x^n]}{h_z} - \frac{\Delta_x[H_z^n]}{h_x}\right) \tag{19}$$

$$E_z^{n+\frac{1}{2}} = E_z^{n-\frac{1}{2}} + \frac{\delta t}{\epsilon_{zz}}\left(\frac{\Delta_x[H_y^n]}{h_x} - \frac{\Delta_y[H_x^n]}{h_y}\right) \tag{20}$$

$$q_s^{n+\frac{1}{2}} = \frac{1-\delta t/2R_pC_s}{1+\delta t/2R_pC_s} q_s^{n-\frac{1}{2}} + \frac{\delta t}{1+\delta t/2R_pC_s}\left(j_s^n + \Delta_z[i_1^n]\right) \tag{21}$$

$$H_x^{n+1} = H_x^n - F(N-1)\left(j_s^{n+1} - j_s^n\right) - \frac{\delta t}{\mu_0}\left(\frac{\Delta_y[E_z^n]}{h_y} - \frac{\Delta_z[E_y^n]}{h_z}\right) \tag{22}$$

$$H_y^{n+1} = H_y^n - \frac{\delta t}{\mu_0}\left(\frac{\Delta_z[E_x^n]}{h_z} - \frac{\Delta_x[E_z^n]}{h_x}\right) \tag{23}$$

$$H_z^{n+1} = H_z^n - \frac{\delta t}{\mu_0}\left(\frac{\Delta_x[E_y^n]}{h_x} - \frac{\Delta_y[E_x^n]}{h_y}\right) \tag{24}$$

$$j_s^{n+1} = j_s^n - \frac{\delta t}{(N-1)(1-F)L_sC_s} q_s^n + \frac{\delta t}{(N-1)(1-F)L_s}\left(\frac{\Delta_y[E_z^n]}{h_y} - \frac{\Delta_z[E_y^n]}{h_z}\right) \tag{25}$$

$$i_1^{n+1} = i_1^n - \frac{\delta t}{h_z L_1 C_s}\Delta_z[q_s^{n+\frac{1}{2}}] \tag{26}$$

References

[1] J.B. Pendry, A.J. Holden, D.J. Robbins, W.J. Stewart, Magnetism from conductors and enhanced nonlinear phenomena, IEEE Trans. Microw. Theory Tech. 47 (1999) 2075–2084.
[2] J.B. Pendry, Negative refraction makes a perfect lens, Phys. Rev. Lett. 85 (2000) 3966–3969.
[3] R.A. Shelby, D.R. Smith, S. Schultz, Experimental verifications of a negative index of refraction, Science 292 (2001) 77–79.
[4] D.R. Smith, J.B. Pendry, J.C.K. Wiltshire, Metamaterials and negative refractive index, Science 305 (2004) 788–792.
[5] S.A. Ramakrishna, Physics of negative refractive index materials, Rep. Prog. Phys. 68 (2005) 449–521.
[6] M.C.K. Wiltshire, J.B. Pendry, I.R. Young, D.J. Larkman, D.J. Gilderdale, J.V. Hajnal, Microstructured magnetic materials for RF flux guiding in magnetic resonance imaging, Science 291 (2001) 849–851.
[7] M.C.K. Wiltshire, J.V. Hajnal, J.B. Pendry, D.J. Edwards, C.J. Stevens, Metamaterial endoscope for magnetic field transfer: near field imaging with magnetic wires, Opt. Express 11 (2003) 709–715.
[8] M.C.K. Wiltshire, R.M. Henkelman, I.R. Young, J.V. Hajnal, Metamaterial yoke for signal reception—an initial investigation, Proc. Intl. Soc. Mag. Reson. Med. 11 (2004) 713.
[9] M. Allard, M.C.K. Wiltshire, J.V. Hajnal, R.M. Henkelman, Improved signal detection with metamaterial magnetic yoke, Proc. Intl. Soc. Mag. Reson. Med. 13 (2005) 871.
[10] M.C.K. Wiltshire, E. Shamonina, I.R. Young, L. Solymar, Experimental and theoretical study of magneto-inductive waves supported by one-dimensional arrays of "Swiss rolls", J. Appl. Phys. 95 (2004) 4488–4493.
[11] K.S. Yee, Numerical solution of initial boundary value problems involving Maxwell's equations in isotropic media, IEEE Trans. Antennas Propag. AP-14 (1966) 302–307.
[12] A. Taflove, S.C. Hagness, Computational electrodynamics: the finite-difference time-domain method, Second ed., Artech House, Boston, 2000.
[13] T. Namiki, A new FDTD algorithm based on alternating-direction implicit method, IEEE Trans. Microw. Theory Tech. 47 (1999) 2003–2007.
[14] S.G. García, T.-W. Lee, S.C. Hagness, On the accuracy of the ADI-FDTD method, IEEE Antennas Wirel. Propag. Lett. 1 (2002) 31–34.
[15] G. Mur, Absorbing boundary conditions for the finite-difference approximation of the time-domain electromagnetic-field equations, IEEE Trans. Electromagn. Compat. 23 (1981) 377–382.
[16] J.-P. Bérenger, A perfectly matched layer for the absorption of electromagnetic waves, J. Comput. Phys. 114 (1994) 185–200.
[17] J.-P. Bérenger, Three-dimensional perfectly matched layer for the absorption of electromagnetic waves, J. Comput. Phys. 127 (1996) 363–379.
[18] M. Ricci, N. Orloff, S.M. Anlage, Superconducting metamaterials, Appl. Phys. Lett. 87 (2005) 034102.